Evolution characteristics of shock pressure wave on the copper target irradiated by far-field laser beams

Xueyun Han, Yufeng Peng and Yi Zhang

College of Physics and Electronic Engineering, Henan Normal University, Xinxiang, 453007, China, hanxueyun126@126.com, yufengp@htu.cn

Abstract. Basing on a positive confocal unstable resonator, the propagation characteristics of laser field are studied by means of fast Fourier transform. The output laser beam is focused on a copper target and generates a plasma plume expanding along the normal to the target surface. Considering the absorption of laser radiation in the copper target, we describe heating and melting of the material by a three-dimensional thermal conductivity model. The spatial and temporal evolutions of the plasma shock wave are investigated as functions of the time passed after the pulse laser irradiation. The results show that the maximum pressure of the plasma shock wave is 8.18 GPa at the time $t = 0.8$ μs after the pulse laser is cut off and then it decreases gradually with increasing time. The maximum pressure decays down to 4.73 GPa at $t = 4.8$ μs.

1. Introduction

In recent decades, there has been a long-standing interest of researchers in developing high-power lasers, including chemical carbon dioxide, oxygen-iodine, diode-pumped solid-state and semiconductor diode lasers, for a variety of applications, including material processing and long-range sensing. Key development goals in the field are high brightness and high efficiency. The output intensity distribution from the high-power lasers is generally annular [1].
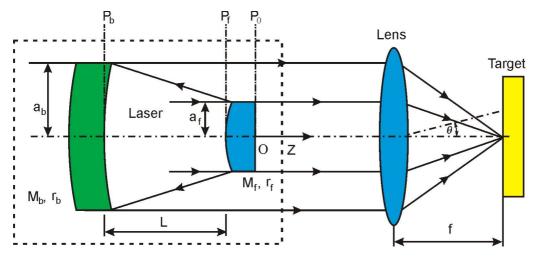
High-intensity nanosecond laser pulses have been used for both fundamental and applied studies for more than two decades, although many of the basic phenomena occurring during laser irradiation of solids have still remained not fully understood. The formation and expansion of a plume produced by laser irradiation of a surface is a starting point for the studies of plume dynamics, ion-assisted film growth and microanalysis. A simple numerical model to describe the main physical processes involved in the laser heating and vaporization of metal targets has been presented by Lunney and Jordan [2]. The model has been used to calculate the plasma absorption, the average ion energy and the ablation depth per pulse for an iron target irradiated with a 26 ns excimer laser pulse at 248 nm. Toftmann et al. [3] have explored experimentally the shape of the plume in the nanosecond laser ablation of metals for different laser beam-spot geometries. Amoruso and Wang [4] have studied the dynamics and composition of the laser ablation plume produced during ultrashort laser irradiation of metals in vacuum. Gacek and Wang [5] have observed the secondary shock wave in the interaction laser–material, and explored the effects of shock-driven process of laser-ablated argon plume in a background gas environment via molecular dynamics simulations. Goh et al. [6] have investigated the expansion dynamics of copper plasma
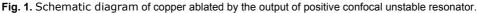
generated via ultrashort laser ablation of pure copper targets by examining optically the plasma plume. Finally, Wang et al. [7] have studied experimentally the plasma plume produced during ultrafast laser ablation of a copper target in high vacuum. Surprisingly, up to now there is no complete theoretical treatment of a time-limited expansion process, even for a neutral expanding plume [3, 8].

In the previous theoretical works for the laser ablation, a mathematical model has generally been artificially predefined to represent specific laser beams, such as Gaussian or flat-topped ones. Basing on the initial built-in oscillation in a laser resonator, a positive confocal unstable resonator with the working wavelength 10.6 μm, in the present work we obtain the intensity and phase distributions for the output laser filed to study the interaction laser–target. Taking into account gas-dynamic continuity equation, Euler equations, N-S equations and energy equations, we establish the two-dimension gas-dynamic calculation model. The spatio-temporal evolutions of the plasma shock wave (PSW) on the copper target are investigated by means of a finite element method, and both the PSW evolution and the flow field distribution are obtained. Therefore the main objectives of the present work are (i) to investigate the absorption of laser radiation on the copper target basing on the initial built-in oscillation in the laser resonator and (ii) to examine the behaviour of the copper plasma plume by means of the finite element methods.

2. Laser field distribution

Schematic diagram of a positive confocal unstable resonator and light propagation is shown in Fig. 1. Here M_b and M_f represent respectively the back and front (output) mirrors of the resonator, r_b and r_f their curvature radii, and a_b and a_f their transverse radii. Of the remaining notation, L means the distance between the mirrors, θ the offset angle of the gravity centre of the far field, and P_b, P_f and P_o the reference planes of the output window. Definitions and numerical values of the parameters involved in our further analysis are listed in Table 1 (see also Ref. [9]).

Fig. 1. Schematic diagram of copper ablated by the output of positive confocal unstable resonator.

The optical wave travelling in a given direction inside the laser resonator may be expressed as $E(x,y,z)\exp(ikz-i\omega t)$, where $E(x,y,z)$ is the amplitude of the laser field, $k=2\pi/\lambda$ the wave vector, λ the wavelength, and ω the angular frequency. The z coordinate increases from inside the front mirror M_f back to the back mirror M_b and then again towards the front mirror. For an

empty resonator, the wave equation for the optical field in rectangular coordinates is given by

$$\frac{\partial^2 \boldsymbol{E}}{\partial \boldsymbol{x}^2} + \frac{\partial^2 \boldsymbol{E}}{\partial \boldsymbol{y}^2} + 2i\boldsymbol{k}\frac{\partial \boldsymbol{E}}{\partial \boldsymbol{z}} = 0. \tag{1}$$

The distribution $E(x, y, 0)$ of the laser field in the plane P_o may be obtained using the fast Fourier transform [9].

Table 1. Definitions and numerical values of the resonator parameters used in our calculations.

Parameter	Magnitude	Unit
Transverse radius of the back mirror a_b	2.40	cm
Transverse radius of the front mirror a_f	1.20	cm
Curvature radius of the back mirror r_b	400	cm
Curvature radius of the front mirror r_f	200	cm
Resonator of length L	100	cm
Geometrical magnification M	2	–
Laser wavelength λ	10.6	μm

3. Model of the shock wave

3.1. Laser heating

Fig. 2 illustrates a copper target ablated by the pulsed laser and a temperature distribution inside the metal target. Here the laser beam is incident along the positive z direction, and the target thickness and radius are equal to d and b, respectively.
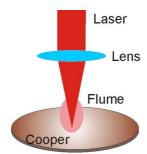

Fig. 2. A scheme of copper target irradiated by a pulsed laser.

We assume that the laser beam consists of plane waves over the light-propagation region in the substrate, while the radius of the laser beam is constant and does not changes along the propagation depth, resulting in a constant cross-section area with respect to z. The light energy is absorbed in a finite depth of the medium bound by the laser light-propagation region, thus causing thermal effects in the target and a temperature increase.

For microsecond pulsed lasers, the thickness of laser transmission is far less than the thermal diffusion thickness. Accordingly, the energy flow from the laser can be considered to form a heat source on the target surface. Let κ be the average thermal conductivity, C the latent heat, ρ the density and $I_s(\boldsymbol{r}, t)$ the net energy flow on the target surface. Then the target-surface temperature

increase T_s can be expressed as [2]

$$T_S(t) = T_0 - \frac{L_F}{C} + \frac{1}{\sqrt{\pi\kappa\rho C}} \int_0^t I_S(\vec{r}, t-\tau) \frac{d\tau}{\sqrt{\tau}}, \qquad (2)$$

where T_0 denotes the initial temperature on the target surface and L_F the thermal capacity.

When the temperature of the target is very high, the thermal conductivity k and the specific heat capacity C of the material can no longer be taken as constants and become temperature-dependent. We use a 3D transient thermal finite-element model to solve the equation for transient heat conduction [10]:

$$\nabla \cdot \left[k\nabla T(\vec{r}, t) \right] + q''(\vec{r}, t) = \rho C_p \frac{\partial T(\vec{r}, t)}{\partial t}, \qquad (3)$$

$$k(T) \frac{\partial T(r, z, t)}{\partial z} \bigg|_{z=0} + hT(r, 0, t) = q''(r, t). \qquad (4)$$

In Eqs. (3) and (4) k implies the thermal conductivity, $T(\vec{r}, t)$ the temperature, $\vec{r}$ the position vector, t the time, ρ the density, h the ideal-gas enthalpy, C_p the specific heat, and q'' the heat generation rate per unit volume. The latter may be described as [2]

$$q'' = (1 - R_L)I_L \exp\left(-\frac{\sigma_p Nl}{\cos\phi}\right) + I_p(1 - R_p) - \left(\frac{d(Nl)}{dt}\right)L_V, \qquad (5)$$

where I_L is the incident laser intensity, ϕ the incident angle, I_P the reflected intensity, and R_L and R_P the reflectivities of the target and the plasma, respectively.

The last item $\left(\frac{d(Nl)}{dt}\right)L_v$ in Eq. (5) represents the heat evaporation, in which L_V is the vaporization heat per atom and $d(Nl)/dt$ the change rate of atomic and ionic numbers in plasma per unit area (Nl). The physical parameters of copper required for calculations are gathered in Table 2.

Table 2. Thermal parameters of copper as reported in Ref. [11].

Temperature, K	Specific heat, J/Kg·K	Thermal conductivity, W/m·K
200	356.1	413
250	374.1	406
300	385	401
350	392.6	396
400	398.6	393
500	407.7	386
600	416.7	379
800	–	366
1000	–	352
1200	–	339

We estimate the temperature of solid and liquid phases with the finite element method. The recession velocity of the ablating surface can be evaluated using a Hertz-Knudsen equation and assuming that the explosive effects are negligible. We consider the plasma plume to be in local thermodynamic equilibrium, so that the energy balance enables one to find the plume temperature,

velocity and pressure distributions under the assumption that the gas expansion from the surface target produces a sonic front. Finally, the plume energy balance is influenced by the energy lost originated from irradiation of the plume and by the amount of laser beam energy reflected from the target surface.

3.2. Shock wave expansion

Since the plasma plume can be considered as ideal gas, the single-flow gas-dynamic equation can be solved for the PSW. It is tempting to assume that the plasma generated by the pulsed laser is ideal, in viscid and compressible fluid. Then the gas-dynamic continuity equation, the Euler equation, the N-S equation and the energy equation can be used to describe the pulsed laser-induced PSW. Notice that the expansion of the PSW just resembles an ideal point explosion [12, 13]. For the convenience of calculations and further analysis, we choose the origin at the centre of the ablated surface and taken the normal to be the PSW propagation direction.

The set of equations consists of conservation equations for the mass, energy and momentum, and the diffusion equation:

$$\frac{\partial \rho}{\partial t} + \nabla \cdot (\rho \vec{v}) = 0 , \tag{6}$$

$$\frac{\partial \rho E}{\partial t} + \nabla \cdot [\vec{v}(\rho E + p)] = \nabla \cdot (k \nabla T + \varphi \vec{v}) + \alpha I_L - R , \tag{7}$$

$$\frac{\partial \rho \vec{v}}{\partial t} + \nabla \cdot (\rho \vec{v} \vec{v}) = \nabla p + \nabla \cdot \varphi + \rho \vec{g} + \vec{F} , \tag{8}$$

$$\frac{\partial \rho Y_i}{\partial t} + \nabla \cdot (\rho \vec{v} Y_i) = \nabla \cdot (\rho D_{i,m} \nabla Y_i) . \tag{9}$$

Here φ is the viscosity tensor,

$$\varphi = \mu[(\nabla \vec{v} + \nabla \vec{v}^T) - \frac{2}{3} \vec{I} \nabla \cdot \vec{v}] , \tag{10}$$

$E = h - p/\rho + 0.5v^2$, E denotes the energy, h the enthalpy, ρ the mass density, p the pressure, Y_i the mass fraction of copper vapour in the gas mixture, c_p the specific heat at constant pressure, $\vec{v}$ the velocity vector, k the thermal conductivity, T the temperature, α the absorption coefficient, I_L the laser intensity, R the radiation loss function, $\vec{g}$ the gravity, $\vec{F}$ the external force, μ the dynamic viscosity, $D_{i,m}$ the diffusion coefficient, and $\vec{I}$ the unit tensor. Note that all the material functions depend on the temperature and mass fraction only.

When the pulsed laser irradiates the copper debris, the plasma is generated on the ablated target. The practical expanding process includes the side propagation of the PSW and the evolution of the flow field along the axial direction. Due to symmetrical distributions of the pressure and the temperature, the flow field can be calculated as a two-dimensional problem. We have solved the above equation set in the axial symmetry, using a commercially available program *Fluent 6.1* [14].

4. Results and discussion

4.1. Shock wave velocity

Issuing from Eqs. (6)–(10), one can obtain the evolution diagrams for the PSW. The contours of the velocity as functions of time are shown in Fig. 3a–e. The PSW reaches its maximum velocity, 116 km/s, at the time $t = 0.8$ µs after the pulse laser is cut off. Afterwards it decreases gradually with increasing time. The maximum velocity decays to 87.9 km/s at the time $t = 4.8$ µs. At

$t = 0.8$ μs the region of the maximum velocity is close by the target surface and then it moves gradually away from the metal surface. At the time $t = 4.8$ μs, the distance between this region and the target surface is about 8 cm.

The interface of the PSW and the undisturbed ambient gas consists of the flowing and undisturbed gases (see Fig. 3a–e). The distance along the normal direction between the outmost layer and the spot centre increases with increasing time.
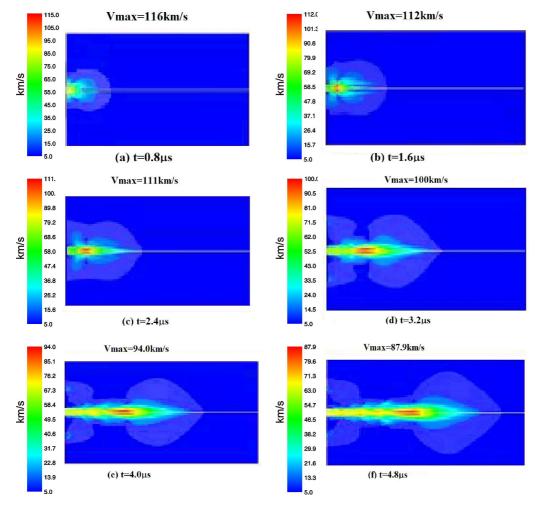

Fig. 3. Calculated contours of velocity for the PSW. (Color online)

4.2. Pressure distributions

The contours of the pressure as functions of time are shown in Fig. 4a–e. One can readily see that the maximum pressure of the PSW is 8.18 GPa. It is achieved at the time $t = 0.8$ μs after the pulse laser is cut off, and then gradually decreases. The maximum pressure decays down to 4.73 GPa at $t = 4.8$ μs.

At the same time moment $t = 0.8$ μs, the spatial region of the maximum pressure is located near the target surface. Then it moves gradually away from the metal surface. The distance between the maximum pressure region and the target surface becomes as large as about 9 cm at $t = 4.8$ μs.

The interface of the PSW and the ambient gas consists of the dynamic pressure and gauge pressure, which is seen from Fig. 3a–e. The distance from the outmost layer to the spot centre along the normal direction increases with increasing time.
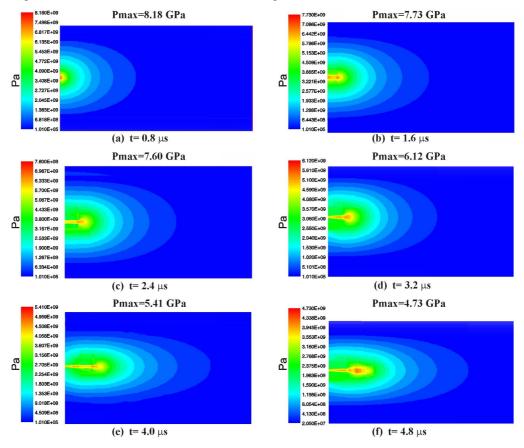

(a) t= 0.8 μs **(b) t= 1.6 μs**

(c) t= 2.4 μs **(d) t= 3.2 μs**

(e) t= 4.0 μs **(f) t= 4.8 μs**

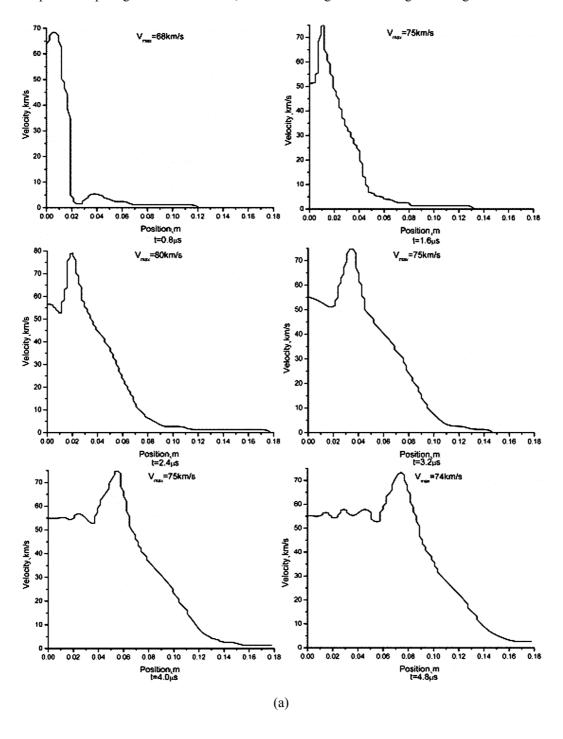**Fig. 4.** Calculated contours of pressure for the PSW. (Color online)

4.3. Axial distributions

In order to understand the propagation characteristics of the PSW in a more detail, we have obtained the relevant spatial distributions along the axial direction shown in Fig. 5a, b. In particular, Fig. 5a illustrates the distribution of velocity in the axial direction, which also coincides with the normal direction. One can see a peak in the corresponding curve, with the velocity at this point being equal to $v \approx 6.8 \times 10^4 \, \text{m/s}$ and the x coordinate being 0.01 m.

If we suppose that the explosion point is on the target surface at the time $t = 0$, then the distance $x = 0.01 \, \text{m}$ implies that it takes $0.8 \, \mu s$ for the centre of the velocity field to move from the laser spot in the normal direction. Passing from Fig. 5a to Fig. 5f, one observes that the summit of the curve becomes lower and lower, and the corresponding x coordinate moves rightwards. This means that the maximum velocity gets lower with time elapse, while the distance to the target surface becomes still farther and farther.

Fig. 5b shows the axial distributions of the pressure induced by the ablated copper debris, with the appropriate parameter values taken the same as in Fig. 4. Here the peak is a core region in the contours of the pressure field. It is reduced with increasing x coordinate so that the peak

becomes farther from the surface of metal target. Notice that the minimum pressure in Fig. 4 is zero, i.e. the overall region corresponds to undisturbed ambient gas whenever the dynamic pressure vanishes. If the dynamic pressure increases above zero, the alternative region of compressed vapour gas is being formed. Finally, one can analyze the distance reached by the compressed vapour gas at different times, when combining the data of Fig. 4 and Fig. 5.
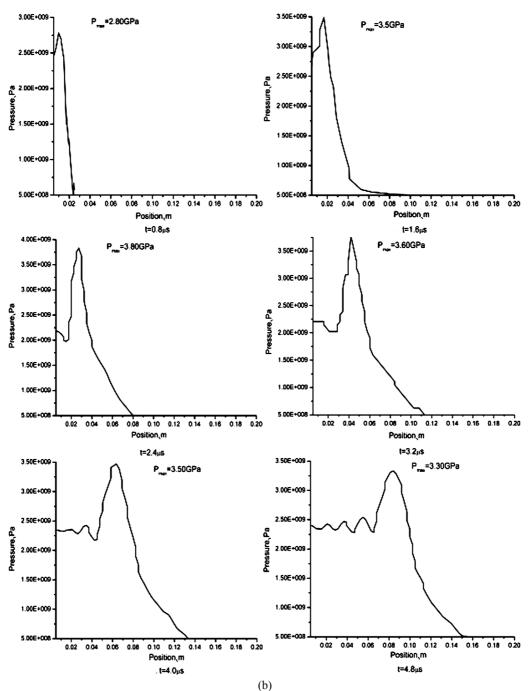

(a)

(b)

Fig. 5. Calculated axial distributions of velocity (a) and pressure (b).

5. Conclusions

As evident from the large number of experimental and theoretical studies carried out on the laser ablation, this subject has attracted significant interest of researchers in the recent years. In the present study we have studied the propagation characteristics of the laser field using the fast Fourier transform and the approach of positive confocal unstable resonator. In particular, we have calculated the spatial and temporal evolutions of the PSW for the case when the far-field output laser beam is focused on a copper target. The spatial velocity, pressure and temperature distributions for

the PSW have been obtained as functions of time passed after the pulse laser radiation is turned off.

It is well known that the laser ablation and propulsion can also be affected by the laser power, the irradiation time, the characteristics of metal targets and some other factors. Therefore in practice the characteristics of the PSWs are determined by many complex factors, which need their further elucidation. Finally, we hope that our results can be helpful for deeper understanding of the influence of laser parameters on the laser ablation and propulsion of space debris.

Acknowledgments

References

1. Davidson N, Friesem A A and Hasman E, 1992. Diffractive elements for annular laser beam transformation. Appl. Phys. Lett. **61**: 381–383.
2. Lunney J G and Jordan R, 1998. Pulsed laser ablation of metals. Appl. Surf. Sci. **127–129**: 941–946.
3. Toftmann B, Schou J and Lunney J G, 2003. Dynamics of the plume produced by nanosecond ultraviolet laser ablation of metals. Phys. Rev. B. **67**: 104101.
4. Amoruso Salvatore and Wang Xuan, 2007. Ultrashort laser ablation of metals. Proc. SPIE. **6604**: 66040.
5. Gacek S. and Wang Xinwei, 2008. Secondary shock wave in laser-material interaction. J. Appl. Phys. **104**: 126101.
6. Goh Y.W., Lu Yongfeng, Hong Minghui and Chong Towchong, 2003. Femtosecond laser ablation of copper. Proc. SPIE. **4830**: 442–446.
7. Wang X, Amoruso S and Xia J, 2009. Temporally and spectrally resolved analysis of a copper plasma plume produced by ultrafast laser ablation. Appl. Surf. Sci. **255**: 5211–5214.
8. Rahman M K, Butt M Z, Mubeen Ishrat and Rafique M S, 2009. Investigation of silver plasma and surface morphology from a nanosecond laser ablation. Mater. Chem. Phys. **114**: 978–982.
9. Peng Yufeng and Liu Li, 2008. Propagation offset characteristics of annular laser beams from confocal unstable resonators through the natural atmosphere. Opt. Commun. **281**: 705–717.
10. Ozisik M N, Heat conduction. New York: John Wiley & Sons (1980).
11. http://www.efunda.com/materials/elements/element_info.cfm?Element_ID=Cu
12. Zhihua Li, Zhang Duanming, Yu Boming and Guan Li, 2002. Characteristics of plasma shock waves generated in the pulsed laser ablation process. Chin. Phys. Lett. **19**: 1841–1843.
13. Leitz K H, Redlingshöfer B, Reg Y, Otto A and Schmidt M, 2011. Metal ablation with short and ultrashort laser pulses. Phys. Procedia. **12**: 230–238.
14. Fluent 6.1 Users Guide. Fluent Inc., Lebanon NH, 2005.

Анотація. За допомогою швидкого перетворення Фур'є в роботі вивчались характеристики лазерного випромінювання додатного конфокального нестійкого резонатора. Лазерне випромінювання фокусувалось на мідній мішені і генерувало плазмовий факел, який поширювався нормально до поверхні мішені. З урахуванням поглинання лазерного випромінювання мідною мішенню, ми описали нагрівання і плавлення матеріалу за допомогою тривимірної моделі теплопровідності. Досліджена просторова і часова еволюція плазмової ударної хвилі як функції часу, що минув після імпульсного лазерного опромінення. Виявлено, що максимальний тиск плазми ударної хвилі становив 8,18 ГПа в момент t = 0,8 мкс після вимкнення лазерного імпульсу і зменшувався з часом, спадаючи до 4,73 ГПа при t = 4,8 мкс.